

Elastic properties of carbonates from laboratory measurements at seismic and ultrasonic frequencies

LUDMILA ADAM and MICHAEL BATZLE, Colorado School of Mines, Golden, USA

Rocks saturated with a fluid can be described as viscoelastic materials. The velocity and elastic moduli of viscoelastic materials increase with frequency. Therefore, the elastic rock properties that we measure at high frequencies might not resemble the observations at lower frequencies. Laboratory measurements of velocity and elastic moduli are mostly performed at frequencies higher than those of surface seismic data, but with the stress-strain experimental procedure the moduli and velocity of laboratory samples can be measured at seismic frequencies.

In this study, we compare measurements at 10 Hz and 0.8 MHz, at reservoir differential pressures, on 11 carbonate samples from the Middle East. We compare how the measurements at these two frequencies probe the sample. We make observations on the dispersion of the different rock properties and effect when performing fluid substitution with Gassmann's relation. And, finally, we will show that for these samples the variation of elastic properties from low to high frequencies is significant. However, if the ratio or difference between dispersive parameters is analyzed, this difference between measurements at different frequencies can be reduced.

The carbonate samples are measured dry and fully saturated with either a light hydrocarbon (liquid butane) or brine (180 000 ppm NaCl) at reservoir differential pressures. Differential pressure is the difference between confining and pore pressure. The samples have a range of porosity, permeability, and textures (labeled A through L in Figure 1).

The moduli and velocities at seismic frequencies (10 Hz) are measured by applying a sinusoidal stress to the rock and measuring the resulting strain in different directions on the rock sample and on the reference material (aluminum). The measured strain amplitudes are at the same scale as for seismic waves ($\sim 10^{-7}$). At ultrasonic frequencies (0.8 MHz), we measure the time of flight of a wave transmitted through the rock sample. From this time, we estimate the P- and S-wave velocities and from these the rock moduli.

The core samples belong to two different reservoirs with a differential pressure of about 35 MPa. Velocity and elastic modulus are measured at a differential pressure (Pd) of 31 MPa for all samples except for sample L, which is measured at a Pd of 24 MPa. For all rocks, pore pressure was constant at 3.5 MPa. The stress-strain system in the laboratory is pressurized with nitrogen gas, but for safety reasons the system is not able to reach the confining pressure of the reservoir. However, the pressures in the experimental setup are close to

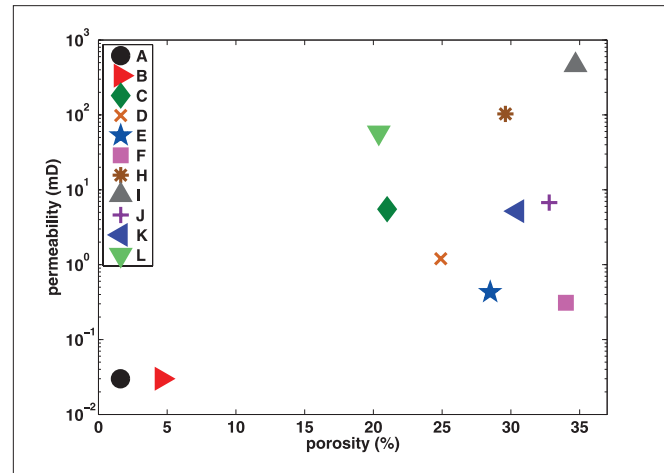


Figure 1. Crossplot of porosity and permeability for the measured carbonate samples.

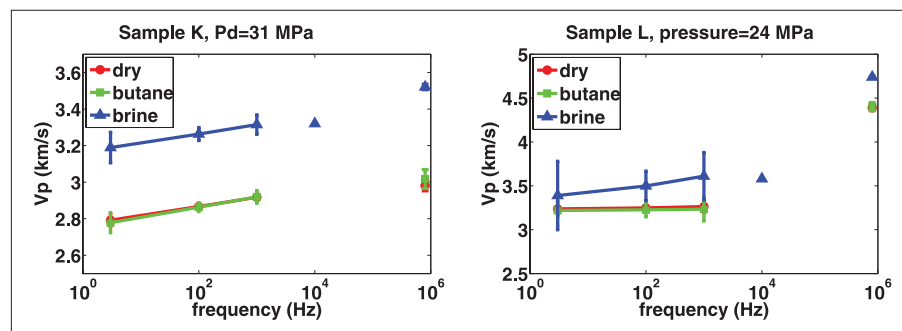


Figure 2. Examples of P-wave velocity dispersion with frequency for samples K and L at a differential pressure of 31 MPa (left) and 24 MPa (right). The samples are dry (humidified) and fully saturated with either liquid butane or brine. Data at 10⁴ Hz are from sonic logs in the cored well.

the reservoir's differential pressure. Most samples are initially humidified to avoid the softening matrix effect of initial introduction of moisture in the pore space. Small amounts of water (less than 1% of the pore volume) can reduce the bulk and shear moduli of the rock significantly. The data in this paper are the estimated mean properties (markers in the plots) and one standard deviation of the random error (error bars in the plots). These values are obtained from a statistical analysis between the measured experimental data and an assumed *true* model. Throughout the paper, the comparisons in modulus and velocity are between the mean values.

Figure 2 shows the P-wave velocity for two samples over a broad frequency band. Three representative points are presented for the low-frequency data (3, 100, and 1000 Hz). The ultrasonic data are collected simultaneously with the low-frequency data at 800 KHz. The data at 10⁴ Hz are obtained from the P-wave sonic log at the same wells and depths from where the rock samples were cored. This velocity is an aver-

age of the velocities from the sonic log over a 0.6-m window centered at the sample depth. Observe in Figure 2 that the velocity estimated at different frequencies is dispersive: The P-wave velocity consistently increases with frequency.

The observation that the velocity at ultrasonic frequency is higher than at seismic frequency can be explained by the viscoelasticity of the material. Alternatively, the ultrasonic wave could be path-dependent, propagating through the fastest path. This preferential higher-velocity path would be a lower-compressibility region of the rock. For example, for partial saturation, the fluid-saturated region is less compressible than the dry region in the rock. However, the ultrasonic data could also be influenced by the combination of both viscoelasticity and path dependence.

There are several rock-fluid mechanisms that describe the viscoelasticity of porous media. Two of the most accepted viscoelastic theories are the Biot and squirt flow mechanisms. For both models, the modulus increases with frequency. Briefly, the passage of a wave stresses the rock creating a fluid movement relative to the rock frame. The fluid is then in an unrelaxed state and would need time to return to its original (prestress) condition. Probing a rock at different frequencies translates into different times that the fluid has to relax. Therefore, the rock properties vary with respect to whether the fluid has had enough time to relax (low frequencies), is completely unrelaxed (high frequencies), or somewhere in between. The specific values of low and high frequencies depend on the fluid and rock properties such as viscosity and permeability.

One of the goals in reservoir characterization is to quantify the fluid content of the rock. The bulk modulus is an intuitive choice to predict fluid content as it describes how resistant a rock is to being compressed, which depends on the amount of fluid in the pore space. Figure 3 shows a partial saturation experiment on sample *L* that compares the bulk modulus estimate at low and high frequency. The bulk modulus increases with the amount of fluid in the pore space. First, observe how the ultrasonic data become sensitive to the brine in the pore space after 20% saturation, while the 10-Hz data do not show stiffening of the rock until 80% saturation. The fluid sensitivity at low saturation can be explained by the ultrasonic wave following a preferential path through the saturated regions in the rock. At 10 Hz, the bulk modulus remains equal to the dry bulk modulus until most pore space is filled with fluid. The stress-strain experiment measures the deformation of the rock sample as a whole. Stress is evenly applied on the rock, and the measured strain is the average of the different locations of the strain sensors. Usually, this type of setup averages the dry and saturated regions in the rock. Therefore, measurements at seismic frequencies are not significantly affected by patchy saturation. The observations at 10 Hz agree with data from producing reservoirs where a small amount of gas (~5%) coming out of solution drops the bulk modulus of the rock close to the dry condition. Dry samples do not exhibit significant dispersion because there is practically no fluid to produce modulus dispersion. The pink arrow at zero saturation (dry) shows the difference between 10 Hz

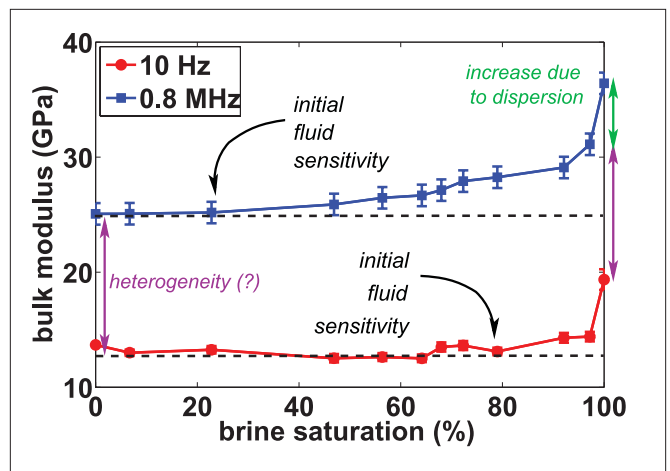


Figure 3. Bulk modulus as a function of brine saturation for sample *L* at seismic and ultrasonic frequencies. The differential pressure is 24 MPa. When the sample is dry (0% saturation), the large difference between 10 Hz and 0.8 MHz is probably caused by sample heterogeneity. At full saturation, this difference is larger, probably due to a combination of heterogeneity and bulk modulus dispersion.

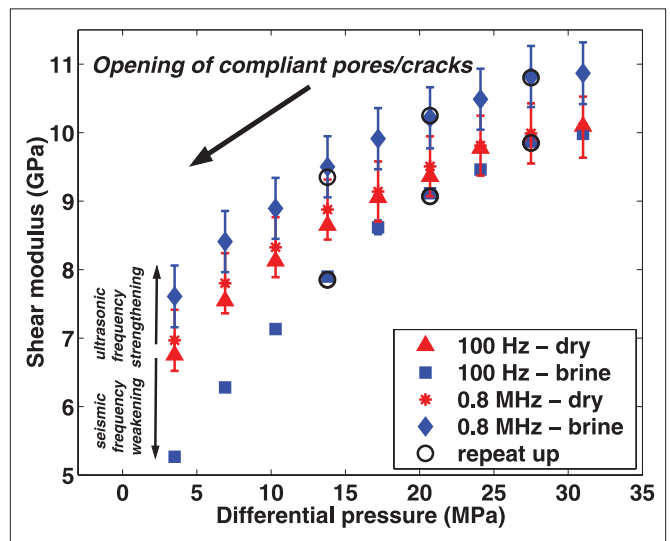


Figure 4. Measurements on sample *C* showing shear modulus weakening and strengthening at seismic and ultrasonic frequencies. Measurements are performed from high- to low-differential pressures. Circles represent repeated differential pressures going from low- to high-differential pressures after the initial unloading cycle was finalized. As we decrease the differential pressure, more compliant pores and cracks open.

and ultrasonic bulk moduli. The higher bulk modulus at ultrasonic frequency is probably caused by a preferential path in the sample rather than modulus dispersion. This sample is significantly heterogeneous with vertical bands of different textures and pore space observed in the X-ray tomographic scan. Most measured samples were generally homogeneous. An arrow of the same length is overlaid at 100% brine saturation, and observe that the difference between 10 Hz and ultrasonic is greater. The remaining difference (green arrow) is possibly caused by rock-fluid mechanisms that cause bulk modulus dispersion.

In most theories, the shear modulus is presumed insen-

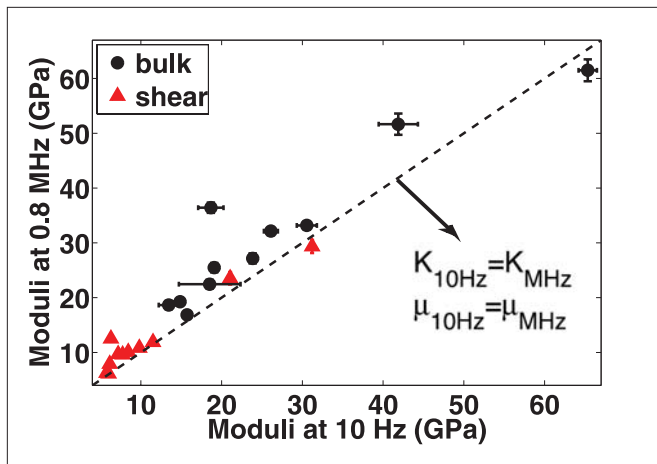


Figure 5. Bulk and shear moduli of carbonate samples at 31 MPa differential pressure and fully brine-saturated. The plot compares measurements at 10 Hz and 0.8 MHz. The dashed line represents where the moduli at both frequencies are equal.

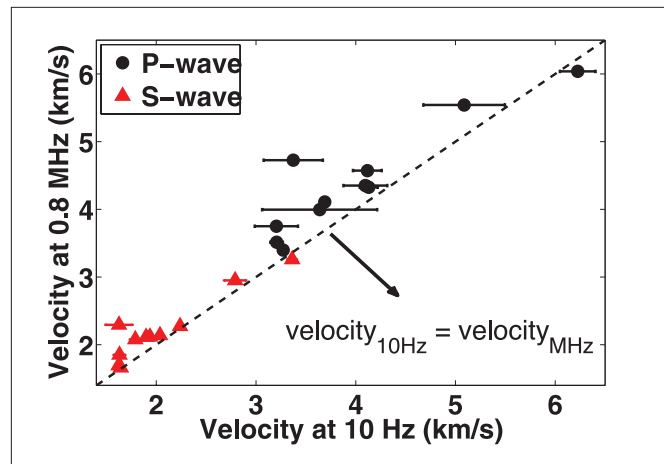


Figure 6. P- and S-wave velocities of carbonate samples at 31 MPa differential pressure and fully brine-saturated. The plot compares measurements at 10 Hz and 0.8 MHz. The dashed line represents where the moduli at both frequencies are equal.

sitive to fluids. However, especially for brine-saturated carbonates, the shear modulus has been observed to increase or decrease with respect to the dry shear modulus (Figure 4). A decrease in the shear modulus from dry to brine saturation could result from the weakening of the solid matrix, possibly associated to the loss of surface energy and/or subcritical crack growth in compliant pores (100-Hz data in Figure 4). Shear modulus dispersion with frequency will show an increase in the shear modulus from dry to brine-saturated conditions (0.8-MHz data in Figure 4). Variations in the shear modulus are more significant at low differential pressures where compliant pores and cracks are open.

Figure 5 shows the bulk and shear modulus for all 100% brine-saturated samples. The dashed line indicates where seismic (10 Hz) and ultrasonic moduli are equal. Observe that for most samples the ultrasonic moduli are greater than the seismic moduli. On average, the moduli increase from 10 Hz to ultrasonic is 23% and 12% for bulk and shear moduli, respectively. The isotropic P-wave velocity depends on the bulk and shear moduli and the rock density. When performing fluid substitution, there will be a trade-off among these parameters affecting the velocity. Figure 6 shows the P- and S-wave velocity for all samples fully saturated with brine at high differential pressure. As expected, the velocity at ultrasonic frequency is greater than the seismic frequency. However, the velocity increase from low- to high-frequency data is on average 9.5% and 5.8% for P- and S-waves, respectively. These lower dispersion values with respect to the moduli result from the trade-offs among rock properties and the definition of the isotropic P-wave velocity (mostly because of the square root in its equation). Nevertheless, the observation that the moduli and the velocities are dispersive for all samples fully saturated with brine holds for the case of full saturation with liquid butane.

If both the P- and S-wave velocities are dispersive, what about the V_p/V_s ratio? Figure 7 shows the V_p/V_s ratio for all samples 100% saturated with butane and brine. For brine, the average increase in the ratio from 10 Hz to ultrasonic is 2.6%;

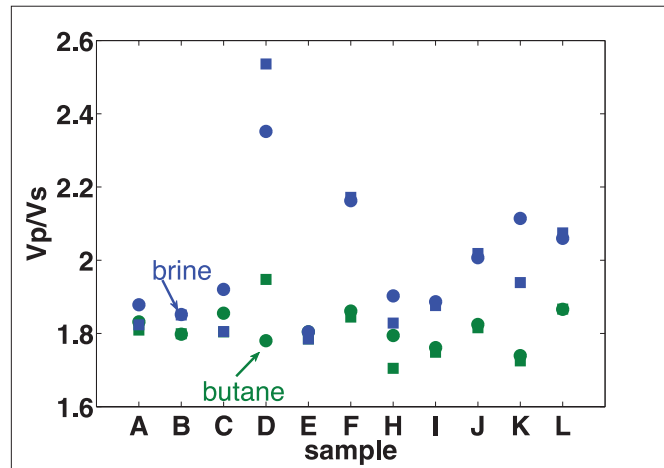


Figure 7. V_p/V_s ratio for the measured samples at 31 MPa differential pressure and fully butane- and brine-saturated. The plot compares measurements at 10 Hz (squares) and 0.8 MHz (circles).

for butane it is 1.9%. Therefore, the velocity dependence on frequency is significantly reduced by taking the ratio of two dispersive parameters.

Laboratory data can be used to perform time-lapse feasibility studies. For example, from the measured velocities, we can compute the impedance and the reflection coefficient to analyze the possible changes in amplitudes resulting from enhanced oil recovery processes in the reservoir. We compute how much the zero-offset P-wave reflection coefficient would change from 10 Hz to 0.8 MHz data, based on the laboratory measurements. We assume that the whole reservoir is represented by the rock properties of one sample and is overlaid by a sandstone layer with a P-wave velocity of 4 km/s and bulk density equal to 2.4 g/cm³ (Figure 8). For a specific fluid, the absolute change in the reflection coefficient amplitude, for example, from seismic to ultrasonic frequency is significant and is on average 0.05 for brine and 0.04 for butane (see for example the arrows in Figure 8, where the arrow size represents this difference for sample L). Let us call the varia-

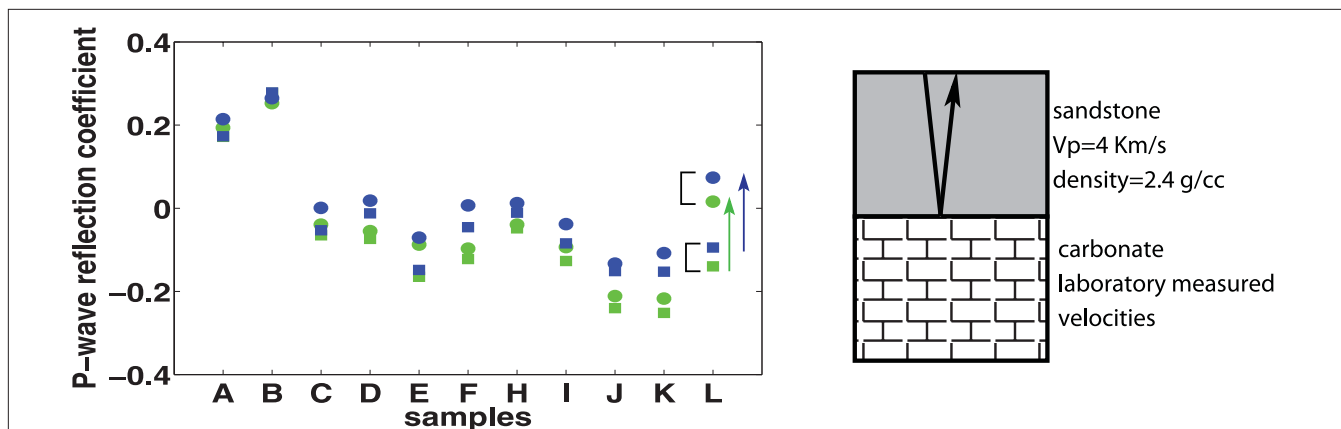


Figure 8. Zero-offset P-wave reflection coefficient for a two-layer reservoir. The bottom layer is represented by the measured samples at 31 MPa differential pressure and either fully saturated with butane (green) or brine (blue). The plot compares measurements at 10 Hz (squares) and 0.8 MHz (circles).

tion in the reflection coefficient from butane to brine ΔRC . If we now look at the absolute values of ΔRC at 10 Hz and at 0.8 MHz, we observe that the difference between seismic and ultrasonic frequencies is smaller than when studying the RC for one fluid (see for example the brackets in Figure 8, where the bracket size represents the ΔRC for sample L). The difference in ΔRC between 10 Hz and 0.8 MHz is on average 0.01. We have to take the absolute value of ΔRC as the RC sign is controlled by the choice of the properties of the top layer. What we can say so far is that for these samples the ultrasonic data agree with the seismic frequency data if the geophysical property is an outcome of the ratio (V_p/V_s) or the difference (ΔRC) of dispersive rock properties. However, when performing quantitative analysis in time-lapse reservoir characterization, our interest focuses on the fluids and their contribution into the rock modulus or velocity. The most well-known equation to study the sensitivity of the rock to fluids is Gassmann's equation:

$$K_{sat} = K_{dry} + \frac{\left(1 - \frac{K_{dry}}{K_{min}}\right)^2}{\frac{\phi}{K_f} + \frac{1-\phi}{K_{min}} - \frac{K_{dry}}{K_{min}^2}} \quad (1)$$

One application for rock physics laboratory data is to verify the validity of Gassmann's relation under different conditions. In the laboratory, we usually measure the modulus for the sample dry (K_{dry}) and saturated with a fluid (K_{sat}). To verify the validity of Gassmann's theory for a set of samples, we compare the measured and computed saturated bulk modulus. We can estimate the saturated modulus with the knowledge of the dry rock modulus, mineral bulk modulus (K_{min}), the porosity (ϕ), and the fluid bulk modulus (K_f). Figure 9 compares the measured and Gassmann-calculated bulk modulus for the samples fully saturated with brine and at the low differential pressure of 3.5 MPa. The line represents the condition at which the measured and Gassmann-estimated bulk modulus are equal. At first glance, note that the ultrasonic data show more samples being accurately predicted by Gassmann's relation. However, Gassmann's theory was derived for zero frequency. This assumption creates a con-

flict between bulk moduli estimated from Gassmann's equation and the measurements at high frequencies. At 10 Hz we observe that fewer samples are accurately predicted by Gassmann's relation. Some reasons for the under- and over-prediction at seismic and ultrasonic frequencies are discussed in Adam et al. (2006) and Baechle et al. (2005). In this paper, we only outline the observations at two frequency ranges. When considering the plots in Figure 9, observe that most samples shift to the right, parallel to the $K_{measured}$ axis. This shift is largely a result of modulus dispersion. We have used Gassmann's theory and the bulk modulus of the dry rock, which is mostly nondispersive, to predict the saturated-rock modulus. However, most of our brine-saturated carbonates show dispersion in the saturated rock bulk modulus. This dispersion results in shifting data points parallel to the measured modulus axis in Figure 9 as the frequency increases from 10 Hz to 0.8 MHz. Figure 10 shows similar plots but at high differential pressure (reservoir pressure). Observe again that at ultrasonic frequency more samples have the bulk modulus accurately predicted by Gassmann than at low frequencies. Although the difference between low and high frequencies is less when the Pd is 3.5 MPa, some samples still show significant modulus dispersion. At high differential pressures, the better prediction of ultrasonic data again results from the dispersion in the measured moduli. Interpreting whether Gassmann is appropriate for carbonates rocks at ultrasonic frequencies could be biased if the measured data in the MHz range are dispersive with respect to the low frequencies, or, even more appropriate, to zero frequency.

The trade-off between bulk and shear moduli and density in the isotropic P-wave velocity equation is also important to consider when studying Gassmann's relation. Consider that in Figure 10, at reservoir differential pressures and 10 Hz, the bulk modulus deviates on average by 14.1% from the line representing perfect prediction by the Gassmann equation. The absolute minimum and maximum deviations for all samples are 0.7% and 35.7%, respectively. If we now analyze the measured and Gassmann-estimated P-wave velocity, the average deviation from perfect prediction is 4.5%, while the absolute minimum and maximum deviations are 0.02% and

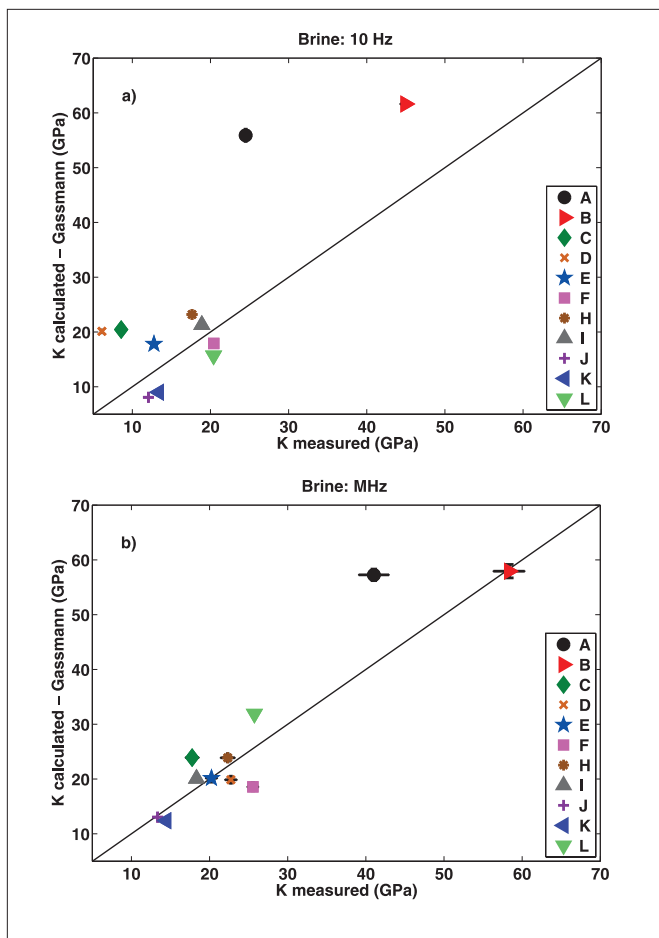


Figure 9. Measured and Gassmann-estimated bulk modulus for the carbonate samples fully saturated with brine at 10 Hz and ultrasonic frequencies. The differential pressure is 3.5 MPa. The line indicates where Gassmann's theory accurately predicts the measured bulk modulus. For some samples, the error bars (one standard deviation) are within the marker size.

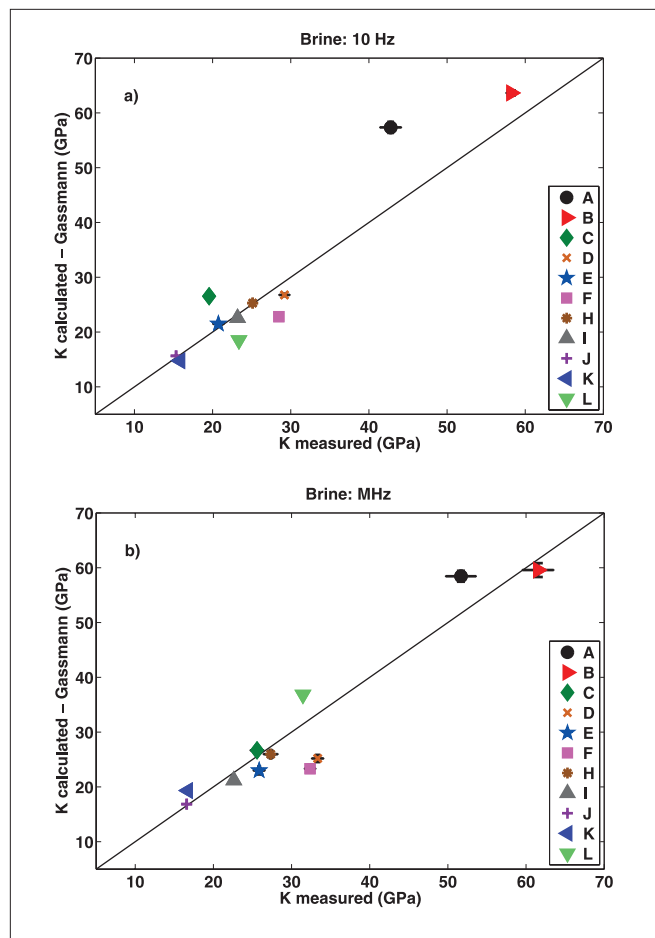


Figure 10. Measured and Gassmann-estimated bulk modulus for the carbonate samples fully saturated with brine at 10 Hz and ultrasonic frequencies. The differential pressure is 31 MPa. The line indicates where Gassmann's theory accurately predicts the measured bulk modulus. For some samples, the error bars (one standard deviation) are within the marker size.

10.3%, respectively. Typically, a 5% deviation in velocity may be considered low, and therefore it might be assumed that Gassmann's theory is valid for these velocity measurements. However, Gassmann's theory was developed for the bulk modulus and zero frequency, and in this domain the deviation is close to 15% for our measured carbonates. Therefore, the variation in the modulus from Gassmann's prediction is more significant than when studying velocities alone. Although in geophysics our main data are velocity and amplitude changes, Gassmann's applicability should probably be analyzed through the bulk modulus rather than the velocity.

In reality, our prime goal in interpreting seismic velocity changes is to identify pore fluid type so that Gassmann's equation can be used to invert for the fluid bulk modulus. A 5% systematic error in velocity or 15% in rock bulk modulus would correspond to a 50% and 200% overprediction in K_{fl} for brine and a light hydrocarbon, respectively. Thus, if we are seeking information on fluid types, dispersion is a serious issue.

Suggested reading. "Gassmann fluid substitution and shear modulus variability in carbonates at laboratory seismic and ultrasonic frequencies" by Adam et al. (GEOPHYSICS, 2006). "Changes of shear moduli in carbonate rocks: Implications for Gassmann applicability" by Baechle et al. (TLE, 2005). "Fluid mobility and frequency-dependent seismic velocity" and "Direct measurements" by Batzle et al. (GEOPHYSICS, 2006). "Variation in dynamic elastic shear modulus of sandstone upon fluid saturation and substitution" by Khazanehdari and Sothcott (GEOPHYSICS, 2003). "To fluid-substitute or not to fluid-substitute: How pore shape and chemical processes affect Gassmann's predictability" by Vanorio et al. (SEG 2007 Expanded Abstracts).

Acknowledgments: We thank ADNOC, ADCO and StatoilHydro for permission to publish the paper, and Kasper van Wijk for suggestions.

Corresponding author: ladam@mines.edu